

## 1

## Polymerization-Induced Self-assembly of Block Copolymer Nano-objects via Green RAFT Polymerization

Shinji Sugihara

*University of Fukui, Graduate School of Engineering, Department of Applied Chemistry and Biotechnology,  
3-9-1 Bunkyo, Fukui 910-8507, Japan*

### 1.1 Introduction

Many biomolecules have specific three-dimensional structures in water or hydrophobic environments, and form higher order structures with high functions. To construct a highly functionalized and higher order structure with a synthetic polymer, it is necessary to examine the fundamental formulation to control the polymer's primary structure and to build the polymers up into a higher order structure. From this point of view, this chapter focuses on block copolymer synthesis as a *molecular technology* for self-organization. The key technology is *in situ* "polymerization-induced self-assembly (PISA)."

### 1.2 Block Copolymer Solution

Self-assembly of AB diblock, ABA, or ABC triblock copolymers to form a variety of macromolecular nanostructures is well known in both the solid state and in dilute solutions, with various prominent functions stemming from the structure [1–21]. In particular, amphiphilic AB diblock copolymers have been demonstrated to form a variety of self-assembled aggregate structures in dilute solutions, where the solvent preferentially solvates one of the blocks. Thus, the basic driving force for solution self-assembly is the solvophobic effect (hydrophobic effect in aqueous solution). These are well documented in other reviews [1–5]. For the amphiphilic AB diblock copolymer in a block-selective solvent, the precise nanostructure, i.e. morphology, is primarily a result of the inherent molecular curvature described by its mean curvature  $H$  and its Gaussian curvature  $K$ , which are given by the two radii of curvatures  $R_1$  and  $R_2$  in Figure 1.1. The curvature is related to the surfactant packing parameter,  $P$ , which is given by Eq. (1.1). The value of  $P$  depends on the relative core-block volume ( $\nu$ ), the effective interfacial area ( $a_0$ ) at the core–shell/solvent interface, and the chain length normal to the

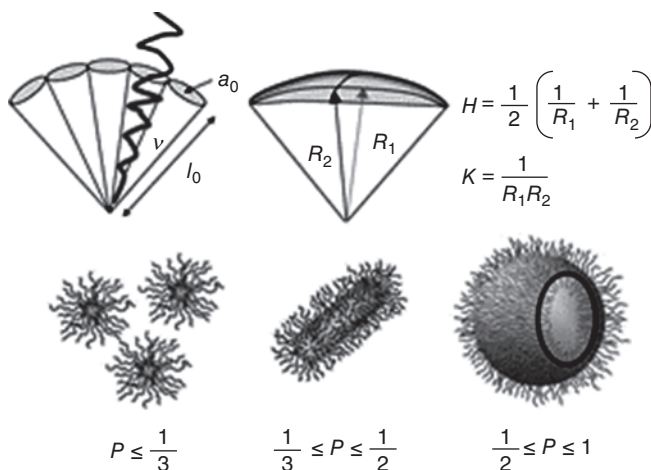


**Figure 1.1** Various self-assemblies formed by solvophilic block copolymers in a block-selective solvent. The type of structure formed is due to the inherent curvature of the molecule, which can be estimated through calculation of its dimensionless packing parameter,  $P$ .

surface per molecule ( $l_0$ ).

$$P = \frac{v}{a_0 l_0} = 1 + Hl_0 + \frac{Kl_0^2}{3} \quad (1.1)$$

The regions of spherical micelles are favored when  $P \leq 0.33$ , cylindrical micelles are produced when  $0.33 < P \leq 0.50$ , and vesicles are formed when  $0.50 < P \leq 1.00$ . Although vesicles are flexible bilayer aggregates, the planar bilayer of lamellae is ideally favored when  $P = 1$ . This concept was originally introduced by Israelachvili et al. [22, 23] to explain self-assembly of small-molecule surfactants, and was later extended to include diblock copolymer self-assembly by Antonietti and Förster [24].

In practice, morphology is controlled by various factors, especially for small-molecule amphiphiles. Assemblies such as spherical micelles, hexagonal, cubes, and lamellar lyotropic crystallines are highly dynamic with rapid exchange of molecules between micelles and the unimer state in solution. Thus, as shown in Figure 1.2, the packing geometry can be tuned by simply adjusting the surfactant concentration with the same solvent properties, i.e. without additives and at a constant temperature. Figure 1.2 shows an ideal phase sequence, which is only a very generalized picture, and the sequence may be different for some amphiphiles. However, this rapid exchange of molecules is very important to determine the structure and morphology of amphiphilic self-assembled aggregates [4, 23–25].

For many macromolecular amphiphiles, in contrast to small-molecule amphiphiles, the rate of exchange of unimers between colloidal aggregates and individual diblock copolymer chains can be negligible, leading to a range of kinetically frozen, i.e. nonergodic, structures. In other words, most amphiphilic

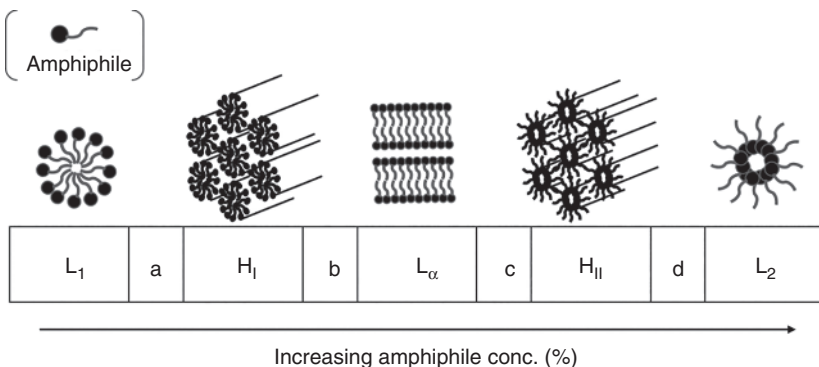


**Figure 1.2** The “ideal” sequence of phases from  $L_1$  to  $H_1$  to  $L_\alpha$  observed upon increasing amphiphile concentration, in a binary small-molecular amphiphile–solvent system (ergodic system). Intermediate phases (a and b) are sometimes observed. The normal micellar structure is termed the  $L_1$  phase. At higher concentrations, micelles can fill space efficiently to form a cubic phase by packing (a). Upon increasing the concentration further, the micelles change from spherical to rod-like ones. The rod-like micelles then pack into a hexagonal ( $H_1$ ) phase. The  $H_1$  phase sometimes changes to a bicontinuous cubic or mesh structure phase (b), which is characterized by nonzero mean curvature and negative Gaussian curvature. The phase then changes to bilayers, which tend to stack into a lamellar phase ( $L_\alpha$ ). Lamellar phases can be found in different phase states including lamellar crystalline, lamellar gel, and lamellar fluid. When the solvent becomes the minority phase, inverse structures are formed such as the inverse hexagonal phase ( $H_{II}$ ), inverse micellar liquid phase ( $L_2$ ), and intermediates such as the inverse bicontinuous phase (c), and inverse micellar cubic phase (d).

block copolymers have been recognized for their many advantages, such as low critical micelle concentration, robust assemblies, and the ability to trap numerous different structures thanks to their kinetic stability due to slow kinetics [4, 26]. For example, this stability of the polymeric micelles is a very important issue for a drug (solubilizing substance) carrier for application in drug delivery systems (DDSs). This is because polymeric micelles can retain the loaded drug in the same morphology for a prolonged period of time even in a very diluted condition in the body [19, 20, 27]. In the early stages of research on DDS, kinetically frozen spherical micelles were used as the drug vehicle. Subsequently, worms (aka cylinders or filomicelles) were found to be better than spherical micelles due to their long circulation time *in vivo* [28, 29] and altered cell internalization pathway compared to spherical constructs [30]. As another example, complex polyprodrug amphiphiles were synthesized from block copolymer amphiphiles, which possess advantages of facile fabrication, high drug loading content and loading stability, active drug protection, blocked premature leakage, and on-demand controlled release [31]. Thus, it is no exaggeration to say that nanoparticles in the biomedical arena are being developed by utilizing the stability of the block copolymer self-organization. Hence, development of the formulation of various self-assemblies is essential and techniques for extracting unstable or metastable assemblies are strongly desired.

### 1.3 Synthesis of Block Copolymers via RAFT Polymerization

In general, controlled/living polymerization refers to chain polymerization without termination and chain-transfer reaction. Since Szawrc discovered living anionic polymerization in 1956 [32, 33], the process has been used in various polymerization mechanisms. In 1962, the first reports on block copolymer self-assembly were published [34]. The advent of controlled/living free-radical polymerization (CRP) [35–38] based on the reversible deactivation of the propagating radicals has revolutionized the domain of polymer chemistry and opened the door to the possibility of designing new polymer architectures and creating new materials with targeted properties. A number of fundamental block copolymers for the assemblies mentioned above have been recently synthesized using controlled/living polymerization techniques, especially CRP.

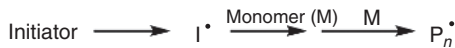
As for CRP, atom transfer radical polymerization (ATRP) [37–40], nitroxide-mediated polymerization (NMP) [41, 42], iodine transfer polymerization (ITP) [43, 44], organotellurium-mediated radical polymerization (TERP) [45, 46], cobalt-mediated radical polymerization (CMRP) [47], reversible addition–fragmentation chain-transfer (RAFT) polymerization [48–50], and reversible chain-transfer-catalyzed polymerization [51, 52] are well known. For almost all polymerizations, the abovementioned PISA has been adopted. Examples of these include ATRP [53–55], NMP [56], ITP [57], and TERP [58, 59]. However, the vast majority of reports at present have focused on the RAFT process, which results in block copolymer formation and self-assembly. Well-documented reviews of this field have been published by Armes and coworkers [60–62], Pan and coworkers [63], Charleux et al. [64], Lowe [65], etc. Incidentally, the author is also one of the coworkers of Prof. Armes.

CRP addresses the philosophy of green chemistry summarized in the 12 main principles that were established by Anastas and Warner in 1998 [66]. CRP meets the criteria of atom economy, and is thus a “green” polymerization [67]. In fact, RAFT polymerization is arguably the most versatile process since it is performed without a metal catalyst, is tolerant to a wide variety of reaction conditions and functionalities, and can be performed on existing conventional free-radical polymerization setups (Scheme 1.1) [48–50]. However, there is a problem of the resulting polymers having undesirable color and odor [68]. RAFT proceeds via a degenerative transfer process and relies on the use of compounds employed as chain-transfer agents such as thiocarbonylthio compounds. The R group initiates the growth of polymeric chains, and the Z group activates the thiocarbonyl bond toward radical addition and stabilizes the resultant adduct radical.

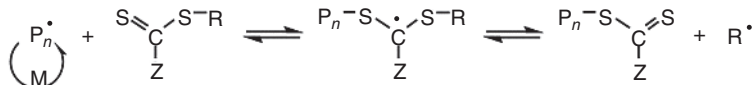
Using such CRP techniques including RAFT polymerization, diblock copolymers for an amphiphile are generally synthesized in good solvent (or bulk) for both blocks. After purification, the desired self-assembly is usually achieved by post-polymerization processing, where solvent quality affects the solubility of the core-forming block. Examples also include self-assemblies in mixtures of good and selective solvents [1–23, 69] and assemblies by stimulus [70–72]. Pioneering work was conducted by Eisenberg’s group over the past two decades,

## Mechanism of RAFT polymerization

## Initiation



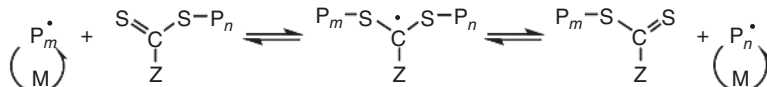
## Reversible chain transfer



## Reinitiation



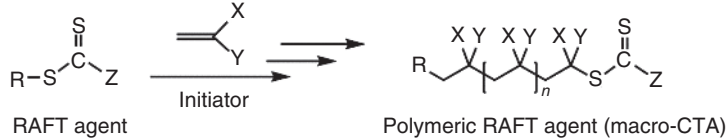
## Chain equilibration



## Termination



## Overall reaction in RAFT polymerization



$$M_{n, \text{calcd}} = \frac{\text{Monomer consumed}}{\text{Chain initiated}}$$

$$(b) \quad \approx \frac{[\text{monomer}]_0}{[\text{RAFT}]_0} \times M_{\text{monomer}} \times \text{convn} + M_{\text{RAFT}} \quad (1.2)$$

**Scheme 1.1** The generally accepted mechanism of RAFT polymerization.

which has established a dominant paradigm for processing block copolymer assemblies in which a common solvent (tetrahydrofuran [THF]) is gradually decreased in quality for one block by addition of a selective solvent (methanol), driving the copolymer to aggregate, as in polystyrene-*b*-poly(acrylic acid) (PSt-*b*-PAA) [12, 13]. Frozen assemblies can also be formed from the block polymer. The formulation is performed as follows. The block copolymer prepared by living anionic polymerization is dissolved in good solvent, *N,N*-dimethyl

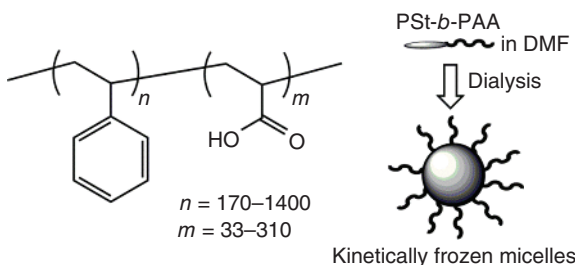


**Figure 1.3** Frozen assembly formation using PSt-*b*-PAA prepared by dialysis against distilled water from DMF solution. The core radii are scaled as  $r_{\text{core}} \sim N_{\text{PSt}}^{0.4} N_{\text{PAA}}^{-0.15}$  (where  $N_{\text{PSt}}$  and  $N_{\text{PAA}}$  are the lengths of the blocks).

formamide (DMF), and then is slowly dialyzed against water (Figure 1.3) [14]. While these assemblies may temporarily be in equilibrium at the onset of aggregation, further addition of the non-solvent pushes the critical aggregation concentration toward zero and drives the solvophobic block to solidify, locking the copolymer into one of a wide range of possible morphologies. However, such processing allows the attainment of only kinetically stable assemblies partly because the polymerization temperature is below the glass transition temperature ( $T_g$ ) of the second block [73], which is typically conducted in highly dilute solutions (<1% solids concentration). Thus, efficient synthesis of block copolymer self-assemblies with well-defined morphologies in concentrated aqueous solution is widely recognized to be a difficult technical challenge. In addition, it is also a formidable challenge to obtain different morphologies without changing the solvent composition from an identical block copolymer that is kinetically frozen.

## 1.4 Polymerization-Induced Self-assembly

### 1.4.1 PISA Using RAFT Process: Emulsion and Aqueous Dispersion Polymerization

To overcome the abovementioned technical challenges, polymerization formulations have been developed using the RAFT process. Initially, Gilbert and coworkers focused on *ab initio* RAFT emulsion polymerization using water-insoluble monomers such as methyl methacrylate and styrene with an amphiphilic macromolecular RAFT agent (the so called “macro-chain-transfer agent [CTA]”) [74]. The amphiphilic macro-CTA can mediate polymerization in both aqueous and organic phases, and is prepared with a water-soluble monomer such as acrylic acid (AA) and a hydrophobic monomer such as *n*-butyl acrylate (BA). The resulting hydrophobic moiety is an oligomer, which forms rigid micelles with a poly(acrylic acid) shell (RAFT-containing seeds). Thus, the self-assembly approach relies on micellar particle nucleation via self-assembly of amphiphilic macro-CTA. This is a very efficient formulation to induce the formation of kinetically trapped spheres (Figure 1.4).

Charleux and coworkers have made considerable progress toward this important scientific objective utilizing various emulsion polymerization formulations. A water-soluble polymer precursor is chain-extended by polymerizing a water-immiscible monomer via living radical polymerization including RAFT so

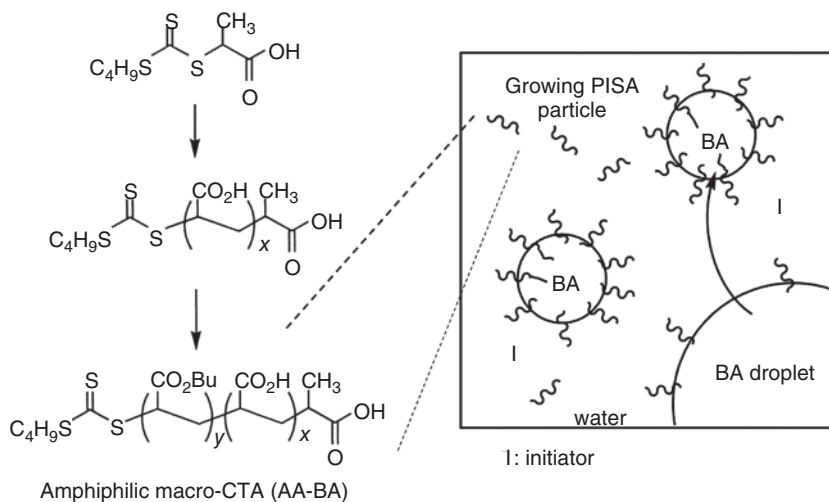


**Figure 1.4** AA-BA-RAFT macro-CTA for RAFT emulsion polymerization of styrene or methyl methacrylate and the *ab initio* RAFT emulsion polymerization model of styrene.

as to produce an amphiphilic diblock copolymer *in situ* [75–78]. This approach leads to PISA and can produce diblock copolymer nanoparticles in the form of spheres, worms, or vesicles, with the final copolymer morphology being dictated primarily by the relative volume fractions of the hydrophilic and hydrophobic blocks. The best advantage of RAFT emulsion polymerization is that many hydrophobic (water-insoluble) monomers are available, unlike the RAFT aqueous dispersion polymerization described below. However, their formation mechanism is complicated because macro-CTA must be sufficiently hydrophobic for micellar nucleation to dominate; otherwise, particles may form mainly via homogeneous nucleation [79, 80].

In contrast to RAFT emulsion polymerization, RAFT dispersion polymerization is a much simpler formulation for self-assembly since the initial reaction solution is homogeneous and block copolymer architecture, such as the packing parameter of the solvent, can be directly applied. An important prerequisite for such formulations is the selection of a water-miscible monomer, which, when polymerized, forms a water-insoluble polymer. Normally, this would simply lead to macroscopic precipitation. However, when using a reactive steric stabilizer (macro-CTA), stable colloidal dispersions can be obtained if an appropriate colloid stability mechanism prevails [81]. This typical formulation using aqueous dispersion polymerization is shown in Figure 1.5.

The first report of RAFT aqueous dispersion polymerization was published by Hawker and coworkers, who prepared poly(*N,N'*-dimethylacrylamide)–poly(*N*-isopropylacrylamide) diblock copolymer (PDMA-*b*-PNIPAM) nanoparticles from PDMA macro-CTA with the aid of microwave irradiation, with the further addition of a bis(acrylamide) cross-linker during the *N*-isopropylacrylamide (NIPAM) polymerization to produce thermoresponsive nanogels as shown in Figure 1.6 [82]. Similar nanogels were prepared in the same year by Charleux

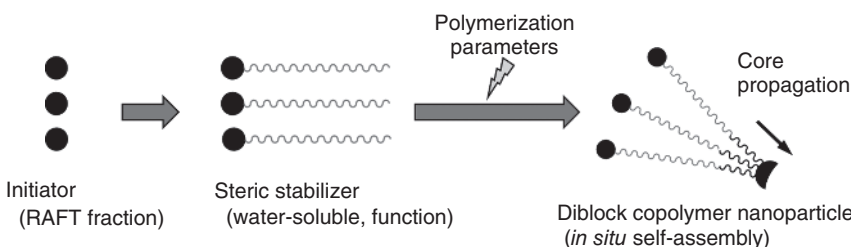


**Figure 1.5** Typical formulation using aqueous dispersion polymerization: a soluble diblock copolymer is initially obtained after the second block copolymerization from a steric stabilizer block, but at some critical degree of polymerization the growing second block becomes water insoluble, which causes *in situ* self-assembly to form a micellar nanoparticle. Upon further polymerization, various morphologies can be formed depending on the polymerization parameters. The primary structural feature governing the final nanoparticle morphology is the packing parameter, i.e. the relative volume fractions of the constituent blocks.

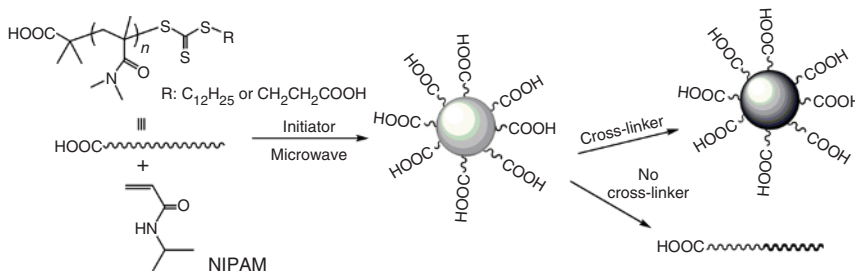


**Figure 1.6** Initial research on RAFT aqueous dispersion polymerization of NIPAM for the synthesis of nanogels.

and coworkers using NMP instead of RAFT polymerization [83]. NMP is also a metal-free polymerization but is available to only a small number of monomers [42].

Recent synthetic advances in RAFT aqueous dispersion polymerization now allow spherical micelles, stable or metastable worm-like micelles or vesicles, and nonspherical strange assemblies composed of well-defined AB diblock copolymers to be prepared directly in concentrated aqueous solution as described in detail later [84–87]. However, there is a limited number of suitable core monomers that possess the requisite “water-miscible monomer” and “water-insoluble polymer” characteristics for the RAFT aqueous dispersion polymerization. This is a pressing issue to solve.

In the case of RAFT dispersion polymerization in a variety of media such as alcohols including alcohol/water mixtures, some core monomers including commodity styrenes can be utilized. The first research on this was reported by Zeng and Pan [88]. Representative examples of other media are polar media [88], non-polar media [89], ionic liquids [90], and supercritical  $\text{CO}_2$  [91]. Reviews of RAFT dispersion polymerization in nonaqueous media are shown in Refs. [64, 65].

### 1.4.2 Reagents for RAFT Aqueous Dispersion Polymerization

Aqueous dispersion (precipitation) polymerization is a heterogeneous polymerization process carried out in the presence of a polymeric stabilizer in a reaction medium using a water-soluble initiator. Thus, in RAFT aqueous dispersion polymerization, a highly hydrated macro-CTA as a steric stabilizer is needed for high dispersion stability with good blocking efficiency. Suitable reagents are listed in Sections 1.4.2.1–1.4.2.3.

#### 1.4.2.1 RAFT Agents

The structure of the RAFT agent is not crucial because most hydrophilic macro-CTAs prepared by RAFT polymerization can be utilized and its influence on a polymer of sufficient molecular weight seems to be small. However, RAFT polymer chain ends are often susceptible to hydrolysis when RAFT polymerizations are conducted in water. In particular, dithiobenzoates are more susceptible to *in situ* hydrolysis than trithiocarbonates [92]. However, commonly used RAFT agents such as dithiobenzoates and trithiocarbonates are available for aqueous dispersion polymerization giving high monomer conversions and good blocking efficiencies. This may be because polymerization proceeds in a waterless field, i.e. a hydrophobic core. As dispersion polymerization progresses, the growing second block becomes a water-insoluble block, which causes *in situ* self-assembly to form a micellar nanoparticle. Thus, the penetration of monomers into the hydrophobic core gradually becomes more difficult, which causes the molecular weight distribution to become larger than in homogeneous polymerization. Since the macro-CTA is required to have high hydrophilicity, carboxylic RAFT agents are often used. However, ionization of the carboxylic acid end group on a shell block derived from the RAFT agent occasionally induces a morphology transition [93].

#### 1.4.2.2 Steric Stabilizer (Macro-CTA, Shell)

The macro-CTA plays both the role of a steric stabilizer block and the function of the resulting block copolymer. In RAFT aqueous dispersion polymerization, a wide range of steric stabilizers are used as shown in Figure 1.7. Most CTAs for shell structures are well documented for both aqueous dispersion and emulsion polymerization [61]. Among them, functional examples include zwitterionic poly(2-(methacryloyloxy)ethylphosphorylcholine) (PMPC) with biocompatibility and enhanced salt tolerance [84, 85, 94], nonionic poly(ethylene oxide) (PEO) with biocompatibility [87, 95], and anionic poly(ammonium 2-sulfatoethyl methacrylate) with the ability to include particles within inorganic crystalline hosts [96], which is used in a 2:1 v/v ethanol/water mixture.

#### 1.4.2.3 Monomers (Core)

The choice of an appropriate monomer is difficult for aqueous dispersion polymerization. Literature examples include NIPAM [82], *N,N'*-diethylacrylamide (DEAA) [97], 2-methoxyethyl acrylate (MEA) [87, 98, 99], 2-hydroxypropyl methacrylate (HPMA) [84–86, 93, 95, 96], and di(ethylene glycol) methyl ether methacrylate (DEGMA) [100] as shown in Figure 1.8. These monomers

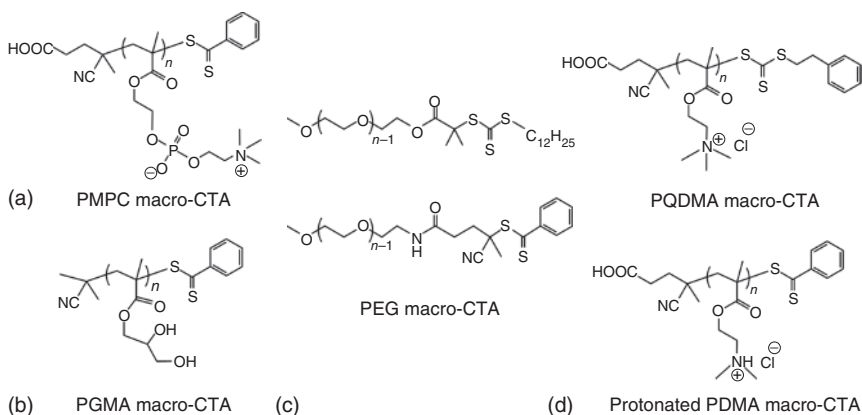


**Figure 1.7** Representative macro-CTAs for RAFT aqueous dispersion polymerization: (a) PMPC, (b) PGMA, (c) polyethylene glycol (PEG), and (d) PQDMA or protonated PDMA.

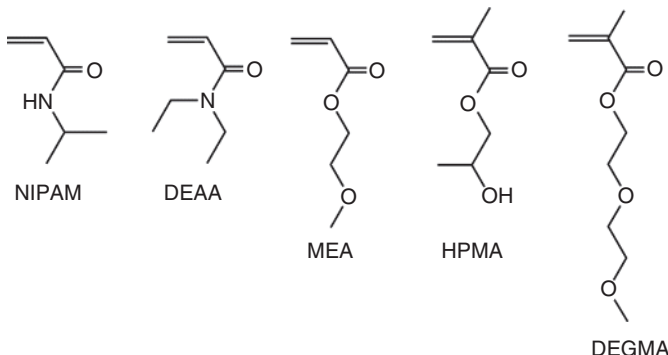


**Figure 1.8** Representative monomers for RAFT aqueous dispersion polymerization.

possess the requisite “water-miscible monomer” and “water-insoluble polymer” characteristics. Strictly speaking, since these monomers have a weakly hydrophobic nature, they produce thermoresponsive polymers that have an appropriate hydrophilic/hydrophobic balanced side chain. For example, lower critical solution temperatures (LCSTs) are approximately 32, 33, under 0, around 0, and 26 °C for NIPAM [101], DEAA [102, 103], MEA [99], HPMA [104], and DEGMA [100, 105], respectively. Since these polymers are synthesized above the LCST, the requisite “water-miscible monomer” and “water-insoluble polymer” characteristics of dispersion polymerization are fulfilled. The weakly hydrophobic nature of the core-forming block leads to interesting thermoresponsive behavior for the assemblies. For example, worms form free-standing gels at room temperature but undergo reversible degelation upon cooling as a result of a worm-to-sphere transition [106, 107]. Analogous thermoresponsive worm gels have also been reported by Monteiro and coworkers [108, 109]. An and coworkers reported tunable sized nanogels using poly(ethylene glycol) methyl ether acrylate prepared via PISA [99, 100], analogous to the initial RAFT aqueous dispersion of NIPAM [82].

### 1.4.3 Representative RAFT Aqueous Dispersion Polymerization

As a representative aqueous dispersion RAFT polymerization, RAFT polymerization of HPMA in water is shown using macro-CTA based on biocompatible PMPC as the solvated block [84, 94]. This formulation is the chain extension of PMPC with HPMA in water, which produces a hydrophobic poly(2-hydroxypropyl methacrylate) (PHPMA) block that drives *in situ* self-assembly to form various assemblies, as shown in Figure 1.9.

Using the same  $\text{PMPC}_{25}$  macro-CTA, various  $\text{PMPC}_{25}-\text{PHPMA}_x$  diblock copolymers were directly prepared in water by varying the total solids content of the formulation. The combined mass of HPMA and  $\text{PMPC}_{25}$  macro-CTA (the mass of the free radical initiator is considered negligible) was initially fixed at 10 wt% solids concentration. Both the  $\text{PMPC}_{25}$  macro-CTA and the HPMA monomer were initially fully soluble in the aqueous reaction solution, but the aqueous dispersion polymerization of HPMA led to *in situ* phase separation and self-assembly, with the final morphology of the  $\text{PMPC}_{25}-\text{PHPMA}_x$  diblock copolymer assemblies dictated solely by the initial reaction conditions. For example, the resulting polymer exclusively formed spherical particle morphologies *in situ* at 10 wt% solids concentration. A systematic increase in the target degree of polymerization (DP) of the PHPMA block from 100 to 400 leads to a monotonic increase in the particle diameter, while maintaining the spherical morphology. It is a common phenomenon that larger spherical morphology is invariably obtained when the chain length of the core-forming block, PHPMA, is increased. This is also well documented in the case of another spherical micellar aggregation formed by diblock copolymers in selective solvents [54, 55, 110].

However, dramatic changes in block copolymer morphology were observed when the aqueous dispersion polymerization of HPMA was conducted under increasingly concentrated conditions, as shown in Figure 1.10. For example, spheres, worms, or vesicles were observed for the  $\text{PMPC}_{25}-\text{PHPMA}_{400}$  series: spheres were obtained at 10% solids concentration, both spheres and worms were obtained at 12.5% and 15%, a pure worm phase was obtained at 16.2%, both worms and vesicles were obtained at 17% and 20%, and purely vesicles were obtained for  $Y \geq 22.5\%$ . The phase diagrams are shown in Figure 1.10, where for a given mean DP of the PMPC block, the final particle morphology obtained at full conversion is solely dictated by (i) the target DP of the PHPMA block and (ii) the total solids concentration at which the HPMA polymerization is conducted. Here, varying the target DP of the PHPMA block at a fixed 25% solids concentration leads to similar morphological control. Thus, for the series of  $\text{MPC}_{25}-\text{PHPMA}_{400}$  at 25 wt% solids, pure phases of spheres, worms, or vesicles were observed. This approach resembles the “ideal” sequence of phases of small-molecular amphiphiles in Figure 1.2 and lipids in nature produced in high concentrations to spontaneously form vesicles. Before this study, literature examples were simply achieved by varying the diblock copolymer composition. The effect of varying the total solids concentration has not been properly explored for such RAFT aqueous dispersion polymerizations.

The mean core width can be controlled by the DP of the core-forming PHPMA chains, as expected from the packing parameter of Figure 1.1. Furthermore,

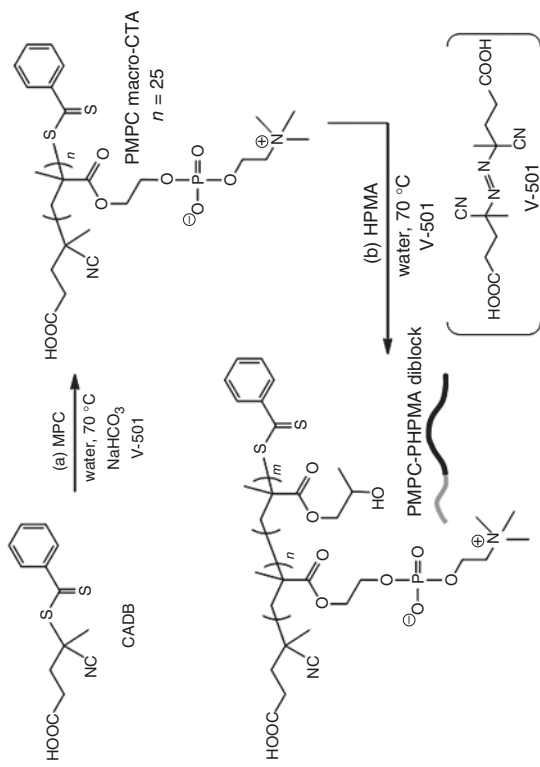
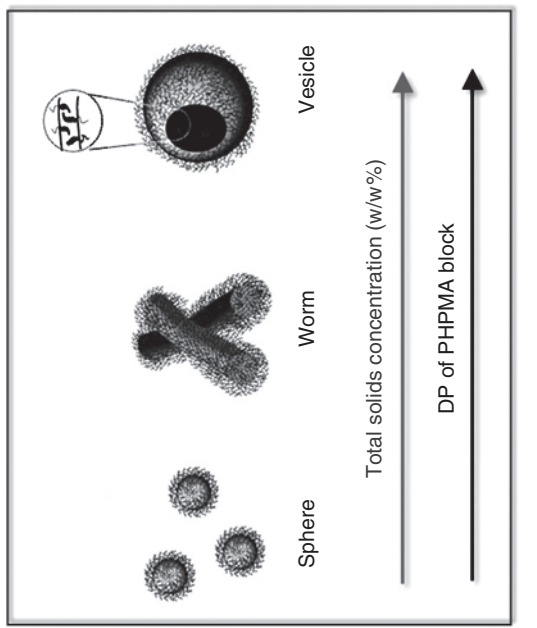


**Figure 1.9** Synthesis of PMPC<sub>25</sub>-*b*-PHPMA<sub>*m*</sub> assemblies via RAFT aqueous dispersion polymerization. Using this facile approach, spheres, worms, or vesicles can be directly prepared, depending on the total solids concentration or the mean degree of polymerization of the PHPMA block.

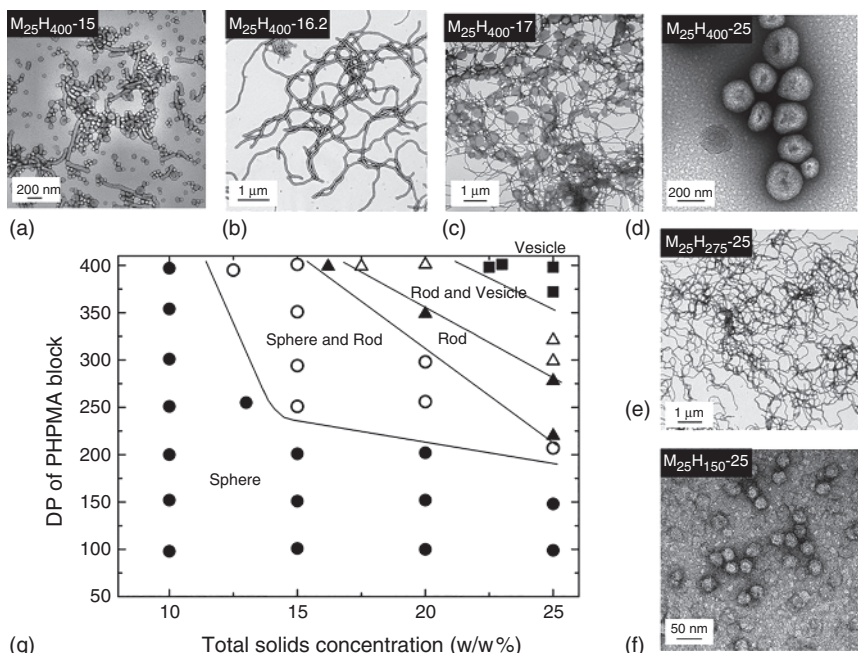


**Figure 1.10** Phase diagram constructed for the  $\text{PMPC}_{25}\text{--PHPMA}_m$  ( $\text{M}_{25}\text{H}_m\text{-Y}$ ) formulation by systematic variation of the mean target degree of polymerization of PHPMA ( $m$ ) and the total solids concentration (Y w/w%) used for each synthesis. Source: Sugihara et al. 2011 [84]. Copyright 2011. Reproduced with permission of American Chemical Society.

the core-forming PHPMA chains within the worms are fully extended, while those of the PHPMA chains within the spheres are intermediate between the fully stretched and fully collapsed states. This information is very important for controlling the formation of various morphologies. In addition, using the phase diagram in Figure 1.10 as a predictive “roadmap” enables the direct, reproducible, and highly efficient preparation of pure phases comprising either block copolymer vesicles or well-defined worms in aqueous solution. For example, metastable worms of toroids or loops can be seen in a detailed kinetic study in the synthesis of  $\text{PMPC}_{25}\text{--PHPMA}_{400}$  at 25% solids concentration.

In this way, the *in situ* self-assembly synthetic route produces frozen, nonergodic structures in aqueous solution. Thus, thanks to this study, two formidable technical challenges of formulation concentrations and different morphologies using identical and kinetically frozen block copolymers were first overcome using RAFT aqueous dispersion polymerization.

In the same period, robust formulations comprising the PHPMA core block and poly(glycerol monomethacrylate) (PGMA) as the hydrophilic stabilizer block were reported by Blanazs et al. [86]. Careful monitoring of the *in situ* polymerization by transmission electron microscopy revealed various novel intermediate structures including branched worms, partially coalesced worms, nascent bilayers, “octopi,” “jellyfish,” and finally pure vesicles that provide

important mechanistic insights regarding the evolution of particle morphology during the sphere-to-worm and worm-to-vesicle transitions.

These two formulations [84, 86] advanced various RAFT aqueous dispersion polymerizations, especially using HPMA. The fundamental polymerization is derived from the size-controllable nanolatexes of PGMA-PHPMA prepared by RAFT aqueous polymerization [111], and the primary polymerization is regarded as a “green” RAFT polymerization [48].

The PHPMA system has been expanded to the PEO-PMEA system [87]. PEO-PMEA diblock copolymers were synthesized by RAFT aqueous dispersion polymerization of MEA using PEO macro-CTA, as shown in Figure 1.11. Both segments are well known to be bio- and blood-compatible polymers. This formulation enables the production of various particle morphologies, such as spheres, worms, and vesicles, from the same block copolymer in water by controlling the solids concentration in the polymerization mixture. As an application for DDS, worms and vesicles are preferable and more efficient in terms of circulation time

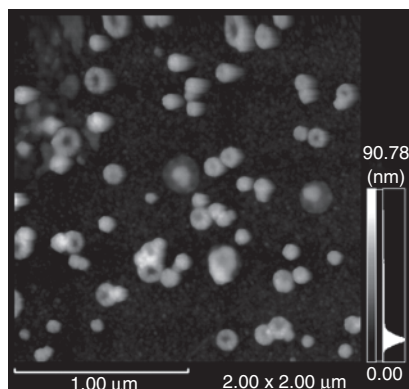
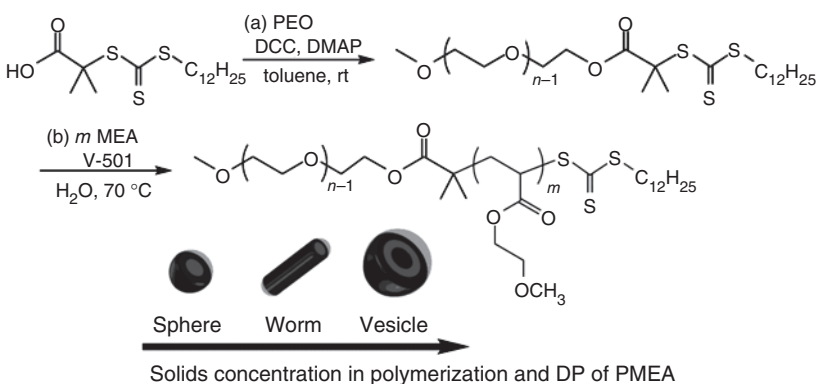


**Figure 1.11** RAFT aqueous dispersion polymerization of MEA using the PEO macro-CTA ( $n = 113$ ) at  $70^\circ\text{C}$ . Various morphologies can be directly prepared, depending on either the total solids concentration or the DP of the PMEA block. The representative AFM (dynamic mode) image of  $\text{PEO}_{113}$ -*b*- $\text{MEA}_{400}$  prepared at 30.0 wt% solids is shown (right).

and cell entry than spherical micelles [28, 29]. Thus, it is anticipated that these PEO-PMEA formulations will be useful for biomedical applications.

As an example of complex shells, Williams et al. utilized a judicious binary mixture of CTAs, nonionic PGMA, and cationic PQDMA for RAFT aqueous dispersion polymerization of PHPMA [112]. Higher cationic character led to the formation of kinetically trapped spheres. This is because more effective electrostatic stabilization prevents sphere–sphere fusion. If a wholly cationic stabilizer is used, only spheres can be obtained [113, 114]. However, using a binary mixture of a nonionic and a cationic stabilizer allows access to cationic spheres, worms, or vesicles. This is because the nonionic stabilizer dilutes the charge density within the coronal layer. In our research introduced in preprint [115], when the whole PQDMA or protonated PDMA is used in the presence of a large amount of NaCl, the resulting assemblies of PQDMA-PHPMA or protonated PDMA-PHPMA allow access to spheres, rods, toroids, or vesicles. Thus, the final morphology can be dictated by the amount of NaCl, as shown in Figure 1.12 [115].

In the study of PGMA/PQDMA-PHPMA [112], the use of 5 mol% PQDMA stabilizer enabled preparation of a 12.5% w/w cationic worm gel that exhibited a zeta potential of +20 mV and a storage modulus of 137 Pa, as demonstrated by variable temperature rheology studies. This worm gel proved to be thermoresponsive: it underwent reversible degelation upon cooling from 25 to 5 °C. Finally, such cationic gels exhibited weak antimicrobial activity toward the pathogen *Staphylococcus aureus*.

For other interesting morphologies such as toroid, octopi, or jellyfish, which are metastable structures, anisotropic particles can be prepared via RAFT aqueous dispersion polymerization [85]. RAFT synthesis is carried out in the presence of a cross-linker as in the PMPC–PHPMA formulation in Figure 1.13, showing the preparation of  $\text{PMPC}_{50}-(\text{PHPMA}_m\text{-}stat\text{-EGDMA}_x)$  ( $m = 100\text{--}400$ ;  $x = 0\text{--}7$ ) diblock copolymer nanoparticles. At either zero or relatively low levels of ethylene glycol dimethacrylate (EGDMA) cross-linker ( $x \leq 2$  for  $m = 400$ ), only spherical morphologies were observed. However, using higher levels of EGDMA ( $x = 6$ , or up to 1.50 mol% based on HPMA) led to increasing particle anisotropy, with

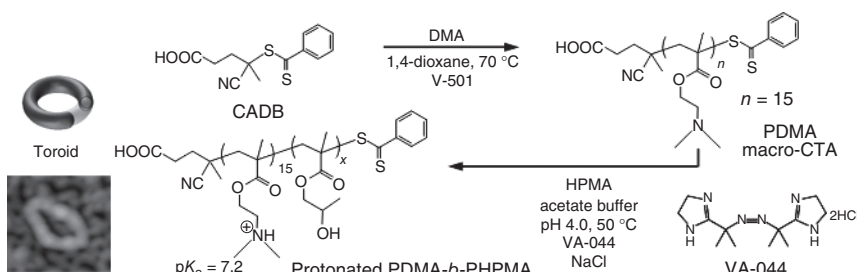


**Figure 1.12** Synthesis of the protonated  $\text{PDMA}_{25}-b\text{-PHPMA}_x$  assemblies via RAFT aqueous dispersion polymerization. Using this facile approach, spheres, rods, toroids, or vesicles can be directly prepared, depending on the amount of  $\text{NaCl}$  at the constant solids. The inset is AFM (dynamic mode) image of a toroid for  $\text{PDMA}_{25}-b\text{-PHPMA}_{300}$  prepared at 25 wt% solids in the presence of 0.13 wt%  $\text{NaCl}$ .

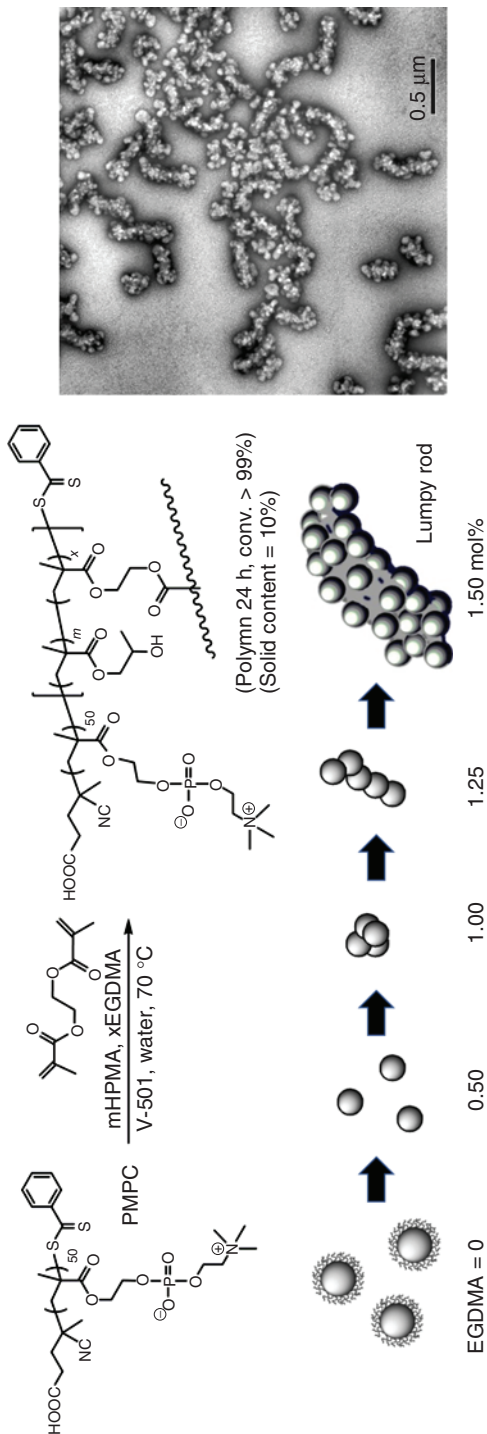


**Figure 1.13** Synthesis of  $\text{PMP}_{50}-(\text{PHPMA}_m-\text{stat-EGDMA}_x)$  nanoparticles with spherical, worm-like, or "lumpy rod" morphologies by RAFT aqueous dispersion polymerization at 70 °C. In each case, the extent of cross-linking dictates the final particle morphology that is obtained.

both a worm-like morphology and a novel “lumpy rod” morphology (comprising fused nano-sized aggregates of primary spherical particles) being observed. In the case of emulsion polymerization for PGMA-PHPMA, the effect of adding a third comonomer such as benzyl methacrylate leads to “frambooidal vesicles.” These morphologies may indicate that the formulations are not dispersion, but seeded, emulsion polymerizations. These may be applied to complex nanocarriers for polyprodrug amphiphiles, as proposed by Liu and coworkers [31].

The formulations and the resulting polymers can be utilized in various fields, e.g. biomedical applications such as DDS [116], and Pickering emulsifiers using worms [117] or vesicles [118] for producing stable oil-in-water emulsions. Such emulsifiers using vesicles are also applied to DNA-mediated self-organization, which leads to interconnected artificial organelles [119]. These assemblies are prepared from the environmentally benign approach of PISA (which involves no toxic solvents, is conducted at relatively high solids concentration, and requires no additional processing) and is readily amenable to industrial scale-up, since it is based on commercially available starting materials.

In addition to RAFT aqueous dispersion polymerization, nonaqueous dispersion polymerization can be applied to toughened epoxy resins with block copolymer worms [17] and films with wrinkly surface patterns [120]. Thus, it is anticipated that these formulations will be useful for both fundamental research and industry.

## 1.5 Promising Polymerization Technology

One of the ultimate goals of PISA using RAFT polymerization is to obtain assemblies of freely controlled morphology. For this purpose, the number of polymers available to serve as steric stabilizers and cores must be increased. As a first step, various synthetic approaches are currently under development in our group. Although radical, cationic, and anionic initiators are used in chain polymerizations of vinyl monomers (strictly speaking, unsaturated monomers), they cannot be used indiscriminately, since all three types of initiation do not work for all vinyl monomers [121]. Monomers show varying degrees of selectivity with regard to the type of reactive center that will cause their polymerization. Most monomers will undergo polymerization with a radical initiator. In other words, RAFT radical polymerization is available for these monomers because it is based on free radical polymerization. In practice, however, among unsaturated monomers, homopolymerization of 1-alkyl alkenes ( $\alpha$ -olefines), 1,1-dialkyl alkenes, vinyl ethers, and aldehydes or ketones cannot be established. Polymers using these building blocks are generally prepared by ionic polymerization, and these monomers except for 1-alkyl alkenes are only amenable to cationic polymerization. Thus, RAFT polymerization of these exclusive cationically polymerizable monomers is an urgent issue. Therefore, we have focused on vinyl ethers, which are typical cationic polymerizable monomers.

To use macro-CTA for RAFT polymerization, well-defined CTA-functionalized polymers are needed and there are several methodologies for their preparation.

These methodologies can be classified into two types of polymerizations: controlled/living cationic polymerization and direct RAFT radical polymerization. The former can also be divided into polymerizations based on termination (**A** and **B**) [110, 122] and initiation methods (**C** and **D**) [123, 124] and those using known living cationic polymerization and novel RAFT cationic polymerization (**E** and **F**) [125, 126] as shown in Figure 1.14. In the case of **A** and **B**, the key to success in the introduction of the RAFT moiety is to utilize a RAFT agent of the carboxylic trithiocarbonate/SnBr<sub>4</sub> initiation system in the presence of an additive such as ethyl acetate or dioxane for living cationic polymerization of vinyl ethers. The living cationic polymerization is initiated from a proton derived from the carboxylic RAFT agent. After a certain period, the polymerization is quenched and the RAFT group as a counteranion is concurrently recovered, followed by the RAFT process of radical polymerization. For **C** and **D**, the living cationic polymerizations of vinyl ethers proceed under the synthesized BVCT-CF<sub>3</sub>COOH adduct/EtAlCl<sub>2</sub> and XTVE-CF<sub>3</sub>COOH adduct/EtAlCl<sub>2</sub> initiating system in the presence of ethyl acetate. Both systems show a living polymerization nature and the resulting polymers have a high number of average end functionality. However, poly(vinyl ether) macro-CTA prepared from carboxylic RAFT agent contains hemiacetal esters as a relatively weak covalent bond for **A** and **B**, and BVCT-HX and XTVE-HX adducts are needed, resulting in a complicated synthesis. In contrast, metal-free RAFT cationic polymerization (MRCP) is also used for *in situ* introduction of the thiocarbonylthio moiety into poly(vinyl ethers). Our group designed a MRCP with RAFT radical and metal-free living cationic polymerizations in the absence of a thiocarbonylthio compound using HCl·Et<sub>2</sub>O [125, 126], and Kamigaito and coworkers used triflic acid as reported by Webster et al. of DuPont in 1990 [127]. This technique enables the production of various block copolymers between radically and cationically polymerizable monomers using both cationic and radical RAFT processes in one pot. Thus, this technique would lead to novel PISA.

Another notable technique is the direct RAFT polymerization of hydroxyl-functional vinyl ethers [128–130]. Although it has been demonstrated that vinyl ethers cannot be inherently homopolymerized via the (controlled) radical mechanism and either no polymer or only oligomers can be obtained via the radical mechanism [131, 132], RAFT radical polymerization has been achieved. The primary key to success in the radical polymerization of vinyl ethers is hydrogen bonding between the vinyl ether oxygen and the hydroxyl group in the pendant of the vinyl ether. This hydrogen bonding reduces the reactivity of the growing radical, suppressing unfavorable side reactions. The resulting hydroxyl-functional vinyl ethers include hydrophilic poly(2-hydroxyethyl vinyl ether), poly(diethylene glycol monovinyl ether), and thermoresponsive poly(4-hydroxybutyl vinyl ether) (LCST  $\sim$  42 °C) [133, 134]. These polymers act as excellent steric stabilizers (macro-CTA) for nanoparticles. Such unprecedented RAFT radical polymerization of vinyl ethers will lead to the synthesis of a wide range of novel copolymers and the development of a radical polymerization system, and eventually “polymerization-induced self-assembly.”

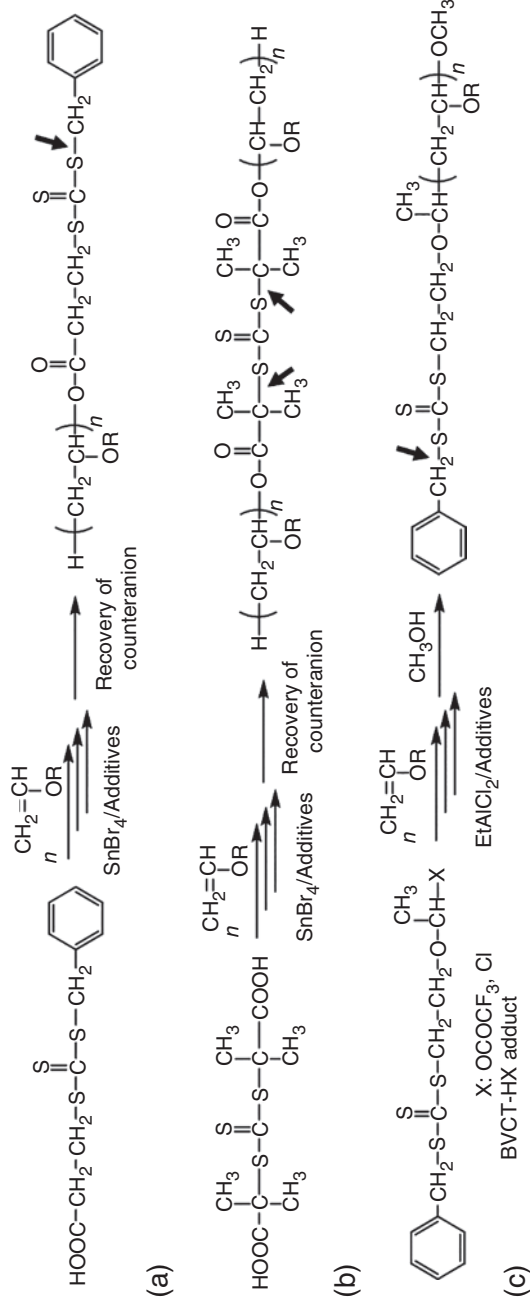


**Figure 1.14** Various syntheses of well-defined chain-transfer agent (CTA)-functionalized poly(vinyl ether)s (macro-CTA), which are candidates for shells of PISA. Arrowed lines denote leaving moieties for RAFT radical polymerization.

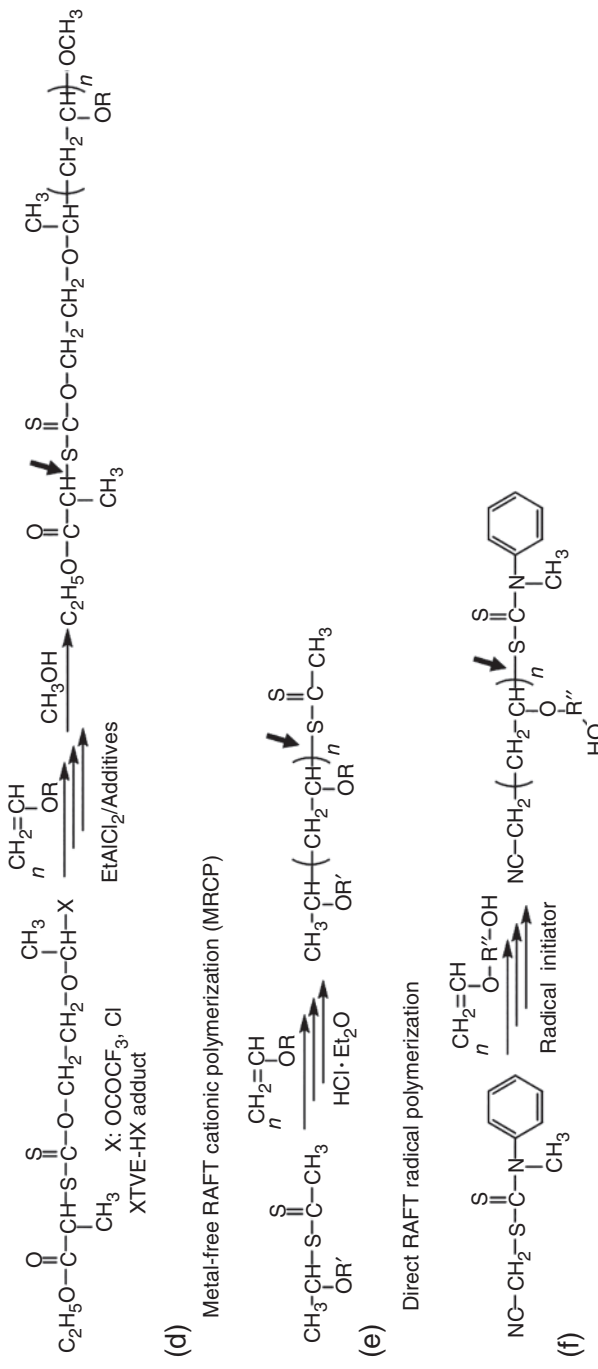


Figure 1.14 (Continued)

## References

- 1 Mai, Y. and Eisenberg, A. (2012). Self-assembly of block copolymers. *Chem. Soc. Rev.* 41 (18): 5969–5985.
- 2 Rodríguez-Hernández, J., Chécot, F., Gnanou, Y., and Lecommandoux, S. (2005). Toward ‘smart’ nano-objects by self-assembly of block copolymers in solution. *Prog. Polym. Sci.* 30 (7): 691–724.
- 3 Bates, F. and Fredrickson, G.H. (1990). Block copolymer thermodynamics: theory and experiment. *Annu. Rev. Phys. Chem.* 41: 525–557.
- 4 Hayward, R.C. and Pochan, D.J. (2010). Tailored assemblies of block copolymers in solution: it is all about the process. *Macromolecules* 43 (8): 3577–3584.
- 5 Blanazs, A., Armes, S.P., and Ryan, A.J. (2009). Self-assembled block copolymer aggregates: from micelles to vesicles and their biological applications. *Macromol. Rapid Commun.* 30 (4–5): 267–277.
- 6 Jain, S. and Bates, F.S. (2003). On the origins of morphological complexity in block copolymer surfactants. *Science* 300 (5618): 460–464.
- 7 Cui, H., Chen, Z., Zhong, S. et al. (2007). Block copolymer assembly via kinetic control. *Science* 317 (5838): 647–650.
- 8 Pochan, D.J., Chen, Z., Cui, H. et al. (2004). Toroidal triblock copolymer assemblies. *Science* 306 (5693): 94–97.
- 9 Hawker, C.J. and Wooley, K.L. (2005). The convergence of synthetic organic and polymer chemistries. *Science* 309 (5738): 1200–1205.
- 10 Won, Y.-Y., Davis, H.T., and Bates, F.S. (1999). Giant wormlike rubber micelles. *Science* 283 (5404): 960–963.
- 11 Gädé, T., Ieong, N.S., Cambridge, G. et al. (2009). Complex and hierarchical micelle architectures from diblock copolymers using living, crystallization-driven polymerizations. *Nat. Mater.* 8 (2): 144–150.
- 12 Discher, D.E. and Eisenberg, A. (2002). Polymer vesicles. *Science* 297 (5583): 967–973.
- 13 Zhang, L. and Eisenberg, A. (1995). Multiple morphologies of “crew-cut” aggregates of polystyrene-*b*-poly(acrylic acid) block copolymers. *Science* 268 (5218): 1728–1731.
- 14 Zhang, L., Barlow, R.J., and Eisenberg, A. (1995). Scaling relations and coronal dimensions in aqueous block polyelectrolyte micelles. *Macromolecules* 28 (18): 6055–6066.
- 15 Discher, B.M., Won, Y.Y., Ege, D.S. et al. (1999). Polymersomes: tough vesicles made from diblock copolymers. *Science* 284 (5417): 1143–1146.
- 16 Wang, H., Wang, X., Winnik, M.A., and Manners, I. (2008). Redox-mediated synthesis and encapsulation of inorganic nanoparticles in shell-cross-linked cylindrical polyferrocenylsilane block copolymer micelles. *J. Am. Chem. Soc.* 130 (39): 12921–12930.
- 17 Liu, J., Thompson, Z.J., Sue, H.-J. et al. (2010). Toughening of epoxies with block copolymer micelles of wormlike morphology. *Macromolecules* 43 (17): 7238–7243.

18 Spulber, M., Nager, A., Winkelbach, K. et al. (2013). Photoreaction of a hydroxyalkyphenone with the membrane of polymersomes: a versatile method to generate semipermeable nanoreactors. *J. Am. Chem. Soc.* 135 (24): 9204–9212.

19 Kataoka, K., Harada, A., and Nagasaki, Y. (2001). Block copolymer micelles for drug delivery: design, characterization and biological significance. *Adv. Drug Delivery Rev.* 47 (1): 113–131.

20 Savic, R., Luo, L.B., Eisenberg, A., and Maysinger, D. (2003). Micellar nanocontainers distribute to defined cytoplasmic organelles. *Science* 300 (5619): 615–618.

21 Torchilin, V.P. (2005). Recent advances with liposomes as pharmaceutical carriers. *Nat. Rev. Drug Discovery* 4 (2): 145–160.

22 Israelachvili, J.N. (1991). *Intermolecular and Surface Forces*. London: Academic Press.

23 Israelachvili, J.N., Mitchell, D.J., and Ninham, B.W. (1976). Theory of self-assembly of hydrocarbon amphiphiles into micelles and bilayers. *J. Chem. Soc., Faraday Trans. 2* 72: 1525–1568.

24 Antonietti, M. and Förster, S. (2003). Vesicles and liposomes: a self-assembly principle beyond lipids. *Adv. Mater.* 15 (16): 1323–1333.

25 Kaasgaarda, T. and Drummond, C.J. (2006). Ordered 2-D and 3-D nanosstructured amphiphile self-assembly materials stable in excess solvent. *Phys. Chem. Chem. Phys.* 8 (43): 4957–4975.

26 Nicolai, T., Colombani, O., and Chassenieux, C. (2010). Dynamic polymeric micelles versus frozen nanoparticles formed by block copolymers. *Soft Matter* 6 (14): 3111–3118.

27 Kataoka, K., Kwon, G.S., Yokoyama, M. et al. (1993). Block copolymer micelles as vehicles for drug delivery. *J. Controlled Release* 24 (1–3): 119–132.

28 Geng, Y., Dalhaimer, P., Cai, S. et al. (2007). Shape effects of filaments versus spherical particles in flow and drug delivery. *Nat. Nanotechnol.* 2: 249–255.

29 Christian, D.A., Cai, S., Garbuzenko, O.B. et al. (2009). Flexible filaments for in vivo imaging and delivery: persistent circulation of filomicelles opens the dosage window for sustained tumor shrinkage. *Mol. Pharmaceutics* 6 (5): 1343–1352.

30 Zhang, K., Rossin, R., Hagooley, A. et al. (2008). Folate-mediated cell uptake of shell-crosslinked spheres and cylinders. *J. Polym. Sci., Part A: Polym. Chem.* 46 (22): 7578–7583.

31 Hu, X., Hu, J., Tian, J. et al. (2013). Polyprodrug amphiphiles: hierarchical assemblies for shape-regulated cellular internalization, trafficking, and drug delivery. *J. Am. Chem. Soc.* 135 (46): 17617–17629.

32 Szwarc, M. (1956). 'Living' polymers. *Nature* 178: 1168–1169.

33 Szwarc, M. (1998). Living polymers. Their discovery, characterization, and properties. *J. Polym. Sci., Part A: Polym. Chem.* 36 (1): IX–XV.

34 Newman, S. (1962). Note on colloidal dispersions from block copolymer. *J. Appl. Polym. Sci.* VI (21): S15–S16.

35 Matyjaszewski, K. and Davis, T. (2002). *Handbook of Radical Polymerization*. Hoboken, NJ: Wiley.

36 Braunecker, W.A. and Matyjaszewski, K. (2007). Controlled/living radical polymerization: features, developments, and perspectives. *Prog. Polym. Sci.* 32 (1): 93–146.

37 Kamigaito, K., Ando, T., and Sawamoto, M. (2001). Metal-catalyzed living radical polymerization. *Chem. Rev.* 101 (12): 3689–3746.

38 Matyjaszewski, K. and Xia, J. (2001). Atom transfer radical polymerization. *Chem. Rev.* 101 (9): 2921–2990.

39 Wang, J.S. and Matyjaszewski, K. (1995). Controlled/“living” radical polymerization. atom transfer radical polymerization in the presence of transition-metal complexes. *J. Am. Chem. Soc.* 117 (20): 5614–5615.

40 Kato, M., Kamigaito, M., Sawamoto, M., and Higashimura, T. (1995). Polymerization of methyl methacrylate with the carbon tetrachloride/dichlorotris-(triphenylphosphine)ruthenium(II)/methylaluminum bis(2,6-di-tert-butylphenoxide) initiating system: possibility of living radical polymerization. *Macromolecules* 28 (5): 1721–1723.

41 Georges, M.K., Veregin, R.P.N., Kazmaier, P.M., and Hamer, G.K. (1993). Narrow molecular weight resins by a free-radical polymerization process. *Macromolecules* 26 (11): 2987–2988.

42 Hawker, C.J., Bosman, A.W., and Harth, E. (2001). New polymer synthesis by nitroxide mediated living radical polymerizations. *Chem. Rev.* 101 (12): 3661–3688.

43 Tatemoto, M. (1992). Development of “iodine transfer polymerization” and its applications to telechelically reactive polymers. *Kobunshi Ronbunshu* 49 (10): 765–783.

44 Matyjaszewski, K., Gaynor, S., and Wang, J.S. (1995). Controlled radical polymerizations: the use of alkyl iodides in degenerative transfer. *Macromolecules* 28 (6): 2093–2095.

45 Yamago, S. (2006). Development of organotellurium-mediated and organostibine-mediated living radical polymerization reactions. *J. Polym. Sci., Part A: Polym. Chem.* 44 (1): 1–12.

46 Yamago, S. (2009). Precision polymer synthesis by degenerative transfer controlled/living radical polymerization using organotellurium, organostibine, and organobismuthine chain-transfer agents. *Chem. Rev.* 109 (11): 5051–5068.

47 Wayland, B.B., Poszmik, G., Mukerjee, S.L., and Fryd, M. (1994). Living radical polymerization of acrylates by organocobalt porphyrin complexes. *J. Am. Chem. Soc.* 116 (17): 7943–7944.

48 Chiefari, J., Chong, Y.K., Ercole, F. et al. (1998). Living free-radical polymerization by reversible addition–fragmentation chain transfer: the RAFT process. *Macromolecules* 31 (16): 5559–5562.

49 Moad, G. (2017). RAFT polymerization to form stimuli-responsive polymers. *Polym. Chem.* 8 (1): 177–219.

50 Barner-Kowollik, C. (ed.) (2008). *Handbook of RAFT Polymerization*. Weinheim: Wiley-VCH.

51 Goto, A., Zushi, H., Hirai, N. et al. (2007). Living radical polymerizations with germanium, tin, and phosphorus catalysts – reversible chain

transfer catalyzed polymerizations (RTCPs). *J. Am. Chem. Soc.* 129 (43): 13347–13354.

52 Goto, A., Hirai, N., Tsujii, Y., and Fukuda, T. (2008). Reversible chain transfer catalyzed polymerizations (RTCPs) of styrene and methyl methacrylate with phosphorus catalysts. *Macromol. Symp.* 261 (1): 18–22.

53 Kagawa, Y., Minami, H., and Okubo, M. (2005). Preparation of block copolymer particles by two-step atom transfer radical polymerization in aqueous media and its unique morphology. *Polymer* 46 (4): 1045–1049.

54 Sugihara, S., Armes, S.P., and Lewis, A.L. (2010). One-pot synthesis of biomimetic shell cross-linked micelles and nanocages by ATRP in alcohol/water mixtures. *Angew. Chem. Int. Ed.* 49 (20): 3500–3503.

55 Sugihara, S., Sugihara, K., Armes, S.P. et al. (2010). Synthesis of biomimetic poly(2-(methacryloyloxy)ethyl phosphorylcholine) nanolatexes via atom transfer radical dispersion polymerization in alcohol/water mixtures. *Macromolecules* 43 (15): 6321–6329.

56 Nicolas, J., Dire, C., Mueller, L. et al. (2006). Living character of polymer chains prepared via nitroxide-mediated controlled free-radical polymerization of methyl methacrylate in the presence of a small amount of styrene at low temperature. *Macromolecules* 39 (24): 8274–8282.

57 Lansalot, M., Farcet, C., Charleux, B. et al. (1999). Controlled free-radical miniemulsion polymerization of styrene using degenerative transfer. *Macromolecules* 32 (22): 7354–7360.

58 Sugihara, Y., Kagawa, Y., Yamago, S., and Okubo, M. (2007). Organotellurium-mediated living radical polymerization in miniemulsion. *Macromolecules* 40 (26): 9208–9211.

59 Kitayama, Y., Chaiyasat, A., and Okubo, M. (2010). Emulsifier-free, organotellurium-mediated living radical emulsion polymerization of styrene. *Macromol. Symp.* 288: 25–32.

60 Derry, M.J., Fielding, L.A., and Armes, S.P. (2016). Polymerization-induced self-assembly of block copolymer nanoparticles via RAFT non-aqueous dispersion polymerization. *Prog. Polym. Sci.* 52: 1–18.

61 Canning, S.L., Smith, G.N., and Armes, S.P. (2016). A critical appraisal of RAFT-mediated polymerization-induced self-assembly. *Macromolecules* 49 (6): 1985–2001.

62 Warren, N.J. and Armes, S.P. (2014). Polymerization-induced self-assembly of block copolymer nano-objects via RAFT aqueous dispersion polymerization. *J. Am. Chem. Soc.* 136 (29): 10174–10185.

63 Sun, J.-T., Hong, C.-Y., and Pan, C.-Y. (2013). Recent advances in RAFT dispersion polymerization for preparation of block copolymer aggregates. *Polym. Chem.* 4 (4): 873–881.

64 Charleux, B., Delaittre, G., Rieger, J., and D'Agosto, F. (2012). Polymerization-induced self-assembly: from soluble macromolecules to block copolymer nano-objects in one step. *Macromolecules* 45 (17): 6753–6765.

65 Lowe, A.B. (2016). RAFT alcoholic dispersion polymerization with polymerization-induced self-assembly. *Polymer* 106: 161–181.

66 Anastas, P.T. and Warner, J.C. (2000). *Green Chemistry: Theory and Practice*, 30. New York: Oxford University Press.

67 Dubé, M.A. and Salehpoor, S. (2014). Applying the principles of green chemistry to polymer production technology. *Macromol. React. Eng.* 8 (1): 7–28.

68 Semsarilar, M. and Perrier, S. (2010). ‘Green’ reversible addition-fragmentation chain-transfer (RAFT) polymerization. *Nat. Chem.* 2 (10): 811–820.

69 Hamley, I.W. (2005). *Block Copolymers in Solution: Fundamentals and Applications*. West Sussex, England: Wiley.

70 Sugihara, S., Ito, S., Irie, S., and Ikeda, I. (2010). Synthesis of thermoresponsive shell cross-linked micelles via living cationic polymerization and UV irradiation. *Macromolecules* 43 (4): 1753–1760.

71 Sugihara, S., Kanaoka, S., and Aoshima, S. (2005). Double thermosensitive diblock copolymers of vinyl ethers with pendant oxyethylene groups: unique physical gelation. *Macromolecules* 38 (5): 1919–1927.

72 Aoshima, S., Sugihara, S., Shibayama, M., and Kanaoka, S. (2004). Synthesis and self-association of stimuli-responsive diblock copolymers by living cationic polymerization. *Macromol. Symp.* 215 (1): 151–164.

73 Zhang, L. and Eisenberg, A. (1998). Formation of crew-cut aggregates of various morphologies from amphiphilic block copolymers in solution. *Polym. Adv. Technol.* 9 (10–11): 677–699.

74 Ferguson, C.J., Hughes, R.J., Pham, B.T.T. et al. (2002). Effective ab initio emulsion polymerization under RAFT control. *Macromolecules* 35 (25): 9243–9245.

75 Rieger, J., Stoffelbach, F., Bui, C. et al. (2008). Amphiphilic poly(ethylene oxide) macromolecular RAFT agent as a stabilizer and control agent in ab initio batch emulsion polymerization. *Macromolecules* 41 (12): 4065–4068.

76 Rieger, J., Osterwinter, G., Bui, C. et al. (2009). Surfactant-free controlled/living radical emulsion (co)polymerization of *n*-butyl acrylate and methyl methacrylate via RAFT using amphiphilic poly(ethylene oxide)-based trithiocarbonate chain transfer agents. *Macromolecules* 42 (15): 5518–5525.

77 Groison, E., Brusseau, S., D’Agosto, F. et al. (2012). Well-defined amphiphilic block copolymer nanoobjects via nitroxide-mediated emulsion polymerization. *ACS Macro Lett.* 1 (1): 47–51.

78 Boursier, T., Chaduc, I., Rieger, J. et al. (2011). Controlled radical polymerization of styrene in miniemulsion mediated by PEO-based trithiocarbonate macromolecular RAFT agents. *Polym. Chem.* 2 (2): 355–362.

79 Ganeva, D.E., Sprong, E., de-Bruyn, H. et al. (2007). Particle formation in ab initio RAFT mediated emulsion polymerization systems. *Macromolecules* 40 (17): 6181–6189.

80 Zetterlund, P.B., Thickett, S.C., Perrier, S. et al. (2015). Controlled/living radical polymerization in dispersed systems: an update. *Chem. Rev.* 115 (18): 9745–9800.

81 Ali, A.M.I., Pareek, P., Sewell, L. et al. (2007). Synthesis of poly(2-hydroxypropyl methacrylate) latex particles via aqueous dispersion polymerization. *Soft Matter* 3 (8): 1003–1013.

82 An, Z., Shi, Q., Tang, W. et al. (2007). Facile RAFT precipitation polymerization for the microwave-assisted synthesis of well-defined, double hydrophilic

block copolymers and nanostructured hydrogels. *J. Am. Chem. Soc.* 129 (46): 14493–14499.

83 Delaittre, G., Save, M., and Charleux, B. (2007). Nitroxide-mediated aqueous dispersion polymerization: from water-soluble macroalkoxyamine to thermosensitive nanogels. *Macromol. Rapid Commun.* 28 (15): 1528–1533.

84 Sugihara, S., Blanazs, A., Armes, S.P. et al. (2011). Aqueous dispersion polymerization: a new paradigm for in situ block copolymer self-assembly in concentrated solution. *J. Am. Chem. Soc.* 133 (39): 15707–15713.

85 Sugihara, S., Armes, S.P., Blanazs, A., and Lewis, A.L. (2011). Non-spherical morphologies from cross-linked biomimetic diblock copolymers using RAFT aqueous dispersion polymerization. *Soft Matter* 7 (22): 10787–10793.

86 Blanazs, A., Madsen, J., Battaglia, G. et al. (2011). Mechanistic insights for block copolymer morphologies: how do worms form vesicles? *J. Am. Chem. Soc.* 133 (41): 16581–16587.

87 Sugihara, S., Ma'Radzi, A.H., Ida, S. et al. (2015). In situ nano-objects via RAFT aqueous dispersion polymerization of 2-methoxyethyl acrylate using poly(ethylene oxide) macromolecular chain transfer agent as steric stabilizer. *Polymer* 76: 17–24.

88 Zheng, G. and Pan, C. (2006). Reversible addition–fragmentation transfer polymerization in nanosized micelles formed in situ. *Macromolecules* 39 (1): 95–102.

89 Fielding, L.A., Derry, M.J., Ladmiral, V. et al. (2013). RAFT dispersion polymerization in non-polar solvents: facile production of block copolymer spheres, worms and vesicles in *n*-alkanes. *Chem. Sci.* 4 (5): 2081–2087.

90 Zhang, B., Yan, X., Alcouffe, P. et al. (2015). Aqueous RAFT polymerization of imidazolium-type ionic liquid monomers: en route to poly(ionic liquid)-based nanoparticles through RAFT polymerization-induced self-assembly. *ACS Macro Lett.* 4 (9): 1008–1011.

91 Jennings, J., Beija, M., Kennon, J.T. et al. (2013). Advantages of block bopolymer synthesis by RAFT-controlled dispersion polymerization in supercritical carbon dioxide. *Macromolecules* 46 (17): 6843–6851.

92 McCormick, C.L. and Lowe, A.B. (2004). Aqueous RAFT polymerization: recent developments in synthesis of functional water-soluble (co)polymers with controlled structures. *Acc. Chem. Res.* 37 (5): 312–325.

93 Lovett, J.R., Warren, N.J., Ratcliffe, L.P.D. et al. (2014). pH-responsive non-ionic diblock copolymers: ionization of carboxylic acid end-groups induces an order–order morphological transition. *Angew. Chem. Int. Ed.* 54 (4): 1279–1283.

94 Sugihara, S. (2012). Synthesis of various block copolymers *via* precision polymerizations with application to nano-organizations. *Kobunshi Ronbunshu* 69 (10): 567–579.

95 Warren, N.J., Mykhaylyk, O.O., Mahmood, D. et al. (2014). RAFT aqueous dispersion polymerization yields poly(ethylene glycol)-based diblock copolymer nano-objects with predictable single phase morphologies. *J. Am. Chem. Soc.* 136 (3): 1023–1033.

96 Ning, Y., Fielding, L.A., Ratcliffe, L.P. et al. (2016). Occlusion of sulfate-based diblock copolymer nanoparticles within calcite: effect of varying the

surface density of anionic stabilizer chains. *J. Am. Chem. Soc.* 138 (36): 11734–11742.

97 Grazon, C., Rieger, J., Sanson, N., and Charleux, B. (2011). Study of poly(*N,N*-diethylacrylamide) nanogel formation by aqueous dispersion polymerization of *N,N*-diethylacrylamide in the presence of poly(ethylene oxide)-*b*-poly(*N,N*-dimethylacrylamide) amphiphilic macromolecular RAFT agents. *Soft Matter* 7 (7): 3482–3490.

98 Liu, G., Qiu, Q., Shen, W., and An, Z. (2011). Aqueous dispersion polymerization of 2-methoxyethyl acrylate for the synthesis of biocompatible nanoparticles using a hydrophilic RAFT polymer and a redox initiator. *Macromolecules* 44 (13): 5237–5245.

99 Liu, G., Qiu, Q., and An, Z. (2012). Development of thermosensitive copolymers of poly(2-methoxyethyl acrylate-*co*-poly(ethylene glycol) methyl ether acrylate) and their nanogels synthesized by RAFT dispersion polymerization in water. *Polym. Chem.* 3 (2): 504–513.

100 Shen, W., Chang, Y., Liu, G. et al. (2011). Biocompatible, antifouling, and thermosensitive core–shell nanogels synthesized by RAFT aqueous dispersion polymerization. *Macromolecules* 44 (8): 2524–2530.

101 Schild, H.G. (1992). Poly(*N*-isopropylacrylamide): experiment, theory and application. *Prog. Polym. Sci.* 17 (2): 163–249.

102 Taylor, L.D. and Cerankowski, L.D. (1975). Preparation of films exhibiting a balanced temperature dependence to permeation by aqueous solutions—a study of lower consolute behavior. *J. Polym. Sci., Part A: Polym. Chem.* 13 (11): 2551–2570.

103 Idziak, I., Avoce, D., Lessard, D. et al. (1999). Thermosensitivity of aqueous solutions of poly(*N,N*-diethylacrylamide). *Macromolecules* 32 (4): 1260–1263.

104 Madsen, J., Armes, S.P., and Lewis, A.L. (2006). Preparation and aqueous solution properties of new thermoresponsive biocompatible ABA triblock copolymer gelators. *Macromolecules* 39 (22): 7455–7457.

105 Lutz, J.-F. (2008). Polymerization of oligo(ethylene glycol) (meth)acrylates: Toward new generations of smart biocompatible materials. *J. Polym. Sci., Part A: Polym. Chem.* 46 (11): 3459–3470.

106 Blanazs, A., Verber, R., Mykhaylyk, O.O. et al. (2012). Sterilizable gels from thermoresponsive block copolymer worms. *J. Am. Chem. Soc.* 134 (23): 9741–9748.

107 Verber, R., Blanazs, A., and Armes, S.P. (2012). Rheological studies of thermo-responsive diblock copolymer worm gels. *Soft Matter* 8 (38): 9915–9922.

108 Jia, Z., Bobrin, V.A., Truong, N.P. et al. (2014). Multifunctional nanoworms and nanorods through a one-step aqueous dispersion polymerization. *J. Am. Chem. Soc.* 136 (16): 5824–5827.

109 Chen, X., Prowse, A.B.J., Jia, Z. et al. (2014). Thermoresponsive worms for expansion and release of human embryonic stem cells. *Biomacromolecules* 15 (3): 844–855.

110 Sugihara, S., Yamashita, K., Matsuzuka, K. et al. (2012). Transformation of living cationic polymerization of vinyl ethers to RAFT polymerization mediated by a carboxylic RAFT agent. *Macromolecules* 45 (2): 794–804.

111 Li, Y. and Armes, S.P. (2010). RAFT synthesis of sterically stabilized methacrylic nanolatexes and vesicles by aqueous dispersion polymerization. *Angew. Chem. Int. Ed.* 49 (24): 4042–4046.

112 Williams, M., Penfold, N.J.W., Lovett, J.R. et al. (2016). Bespoke cationic nano-objects via RAFT aqueous dispersion polymerization. *Polym. Chem.* 7 (23): 3864–3873.

113 Boisse, S., Rieger, J., Belal, K. et al. (2010). Amphiphilic block copolymer nano-fibers via RAFT-mediated polymerization in aqueous dispersed system. *Chem. Commun.* 46 (11): 1950–1952.

114 Semsarilar, M., Ladmiral, V., Blanazs, A., and Armes, S.P. (2013). Cationic polyelectrolyte-stabilized nanoparticles via RAFT aqueous dispersion polymerization. *Langmuir* 29 (24): 7416–7424.

115 Tomoyasu, Y., Sugihara, S., Ma'Radzi, A.H., and Maeda, Y. (2013). In situ formation of vesicle containing amino groups via RAFT aqueous dispersion polymerization. *Polymer Preprint Japan* 62 (2): 2415.

116 Karagoz, B., Esser, L., Duong, H.T. et al. (2014). Polymerization-induced self-assembly (PISA) – control over the morphology of nanoparticles for drug delivery applications. *Polym. Chem.* 5 (2): 350–355.

117 Thompson, K.L., Mable, C.J., Cockram, A. et al. (2014). Are block copolymer worms more effective Pickering emulsifiers than block copolymer spheres? *Soft Matter* 10 (43): 8615–8626.

118 Thompson, K.L., Chambon, P., Verber, R., and Armes, S.P. (2012). Can polymersomes form colloidosomes? *J. Am. Chem. Soc.* 134 (30): 12450–12453.

119 Liu, J., Postupalenko, V., Lörcher, S. et al. (2016). DNA-mediated self-organization of polymeric nanocompartments leads to interconnected artificial organelles. *Nano Lett.* 16 (11): 7128–7136.

120 Guo, L., Jiang, Y., Chen, S. et al. (2014). Self-assembly of poly(methacrylic acid)-*b*-poly(butyl acrylate) amphiphilic block copolymers in methanol via RAFT polymerization and during film formation for wrinkly surface pattern. *Macromolecules* 47 (1): 165–174.

121 Odian, G. (2004). *Principles of Polymerization*, 4e, 200. Hoboken, NJ: Wiley.

122 Sugihara, S., Iwata, K., Miura, S. et al. (2013). Synthesis of dual thermoresponsive ABA triblock copolymers by both living cationic vinyl polymerization and RAFT polymerization using a dicarboxylic RAFT agent. *Polymer* 54 (3): 1043–1052.

123 Ma'Radzi, A.H., Sugihara, S., Miura, S. et al. (2014). Synthesis of thermoresponsive block and graft copolymers via the combination of living cationic polymerization and RAFT polymerization using a vinyl ether-type RAFT agent. *Polymer* 55 (8): 1920–1930.

124 Ma'Radzi, A.H., Sugihara, S., Toida, T., and Maeda, Y. (2014). Synthesis of polyvinyl alcohol stereoblock copolymer via the combination of living cationic polymerization and RAFT/MADIX polymerization using xanthate with vinyl ether moiety. *Polymer* 55 (21): 5332–5345.

125 Sugihara, S., Konegawa, N., and Maeda, Y. (2015). HCl·Et<sub>2</sub>O-catalyzed metal-free RAFT cationic polymerization: one-pot transformation from metal-free living cationic polymerization to RAFT radical polymerization. *Macromolecules* 48 (15): 5120–5131.

126 Sugihara, S., Okubo, S., and Maeda, Y. (2016). Metal-free RAFT cationic polymerization of *p*-methoxystyrene with HCl·Et<sub>2</sub>O using a xanthate-type RAFT cationogen. *Polym. Chem.* 7 (44): 6854–6863.

127 Uchiyama, M., Satoh, K., and Kamigaito, M. (2015). Cationic RAFT polymerization using ppm concentrations of organic acid. *Angew. Chem. Int. Ed.* 54 (6): 1924–1928.

128 Sugihara, S., Kawamoto, Y., and Maeda, Y. (2016). Direct radical polymerization of vinyl ethers: reversible addition fragmentation chain transfer polymerization of hydroxy-functional vinyl ethers. *Macromolecules* 49 (5): 1563–1574.

129 Sugihara, S., Yoshida, A., Fujita, S., and Maeda, Y. (2017). Design of hydroxy-functionalized thermoresponsive copolymers: improved direct radical polymerization of hydroxy-functional vinyl ether. *Macromolecules* 50 (21): 8346–8356.

130 Sugihara, S., Sudo, M., Hirogaki, K., Irie, S., and Maeda, Y. (2018). Synthesis of various poly(2-hydroxyethyl vinyl ether)-stabilized latex particles via surfactant-free emulsion polymerization in water. *Macromolecules* 51 (4): 1260–1271.

131 Kamachi, M., Tanaka, K., and Kuwae, Y. (1986). ESR studies on radical polymerization of vinyl ethers. *J. Polym. Sci., Part A: Polym. Chem.* 24 (5): 925–929.

132 Kumagai, T., Kagawa, C., Aota, H. et al. (2008, 2008). Specific polymerization mechanism involving  $\beta$ -scission of mid-chain radical yielding oligomers in the free-radical polymerization of vinyl ethers. *Macromolecules* 41 (20): 7347–7351.

133 Sugihara, S., Hashimoto, K., Matsumoto, Y. et al. (2003). Thermosensitive polyalcohols: synthesis via living cationic polymerization of vinyl ethers with a silyloxy group. *J. Polym. Sci., Part A: Polym. Chem.* 41 (21): 3300–3312.

134 Sugihara, S., Ohashi, M., and Ikeda, I. (2007). Synthesis of fine hydrogel microspheres and capsules. *Macromolecules* 40 (9): 3394–3401.

